

Calculations of Ice Crystal Growth

K. O. L. F. JAYAWEERA¹

Division of Radiophysics, CSIRO, Sydney, Australia

(Manuscript received 11 November 1969, in revised form 4 November 1970)

ABSTRACT

The growth rates, and the masses to which the crystals grow at different times, are calculated for various temperatures using the electrostatic analogy and assuming that the crystals follow the experimentally observed growth modes. The additional contribution to growth due to ventilation of the falling crystal is calculated. For small plate-like crystals and for all sizes of columns it is comparable with the growth by diffusion alone, while for larger plate-like crystals ventilation predominates.

Peaks in the growth rate occur at temperatures of about -5 and -15°C as a consequence of the high axial ratio of the crystals characteristic of these temperatures (needles and dendrites, respectively). At other temperatures, calculated growth rates do not differ widely from those obtained by assuming a spherical ice particle.

1. Introduction

Experimental determinations of the growth rates for freely falling ice crystals have been made by many authors. Most of these measurements have been confined to particular temperatures and comparatively

short growth times. The available data are summarized in Fig. 1.

It is obvious from this figure that the experimental observations give a very incomplete picture of how growth rate varies with temperature and growth time. We may, however, make two generalizations:

1) The growth rate of an ice crystal at a particular temperature increases with the growth time.

2) There is some indication of peaks in the growth rate at about -5 and -15°C . This is supported by Hallett's (1965) curve of relative growth rates derived from a study of ice crystals growing on a fiber in a diffusion cloud chamber.

For a more complete picture of the growth of ice crystals from vapor, it is necessary to turn to computation. In the past, two methods have been used. The first, exemplified in the work of Todd (1964), relies upon experimental data on the axial growth rates and fits empirical equations to these. Unfortunately, because of the inadequacy of the experimental determinations, this approach involves too many assumptions and extrapolations to be used with confidence.

The second method, first applied to the growth of ice crystals by Houghton (1950), is known as the electrostatic analogy method. The diffusion field surrounding the crystal is analogous to the electrostatic field surrounding a charged conductor, since both satisfy Laplace's equation. The crystal is assumed to have a uniform vapor pressure over its surface equal to the equilibrium vapor pressure, i.e., the surface is ice at a uniform temperature. This assumption has been justified by McDonald (1963). Since analogous boundary conditions exist for geometrically similar bodies, the rate of vapor flux toward the crystal can be calculated for simple shapes of which the electrostatic capacities are known. Comparison between such

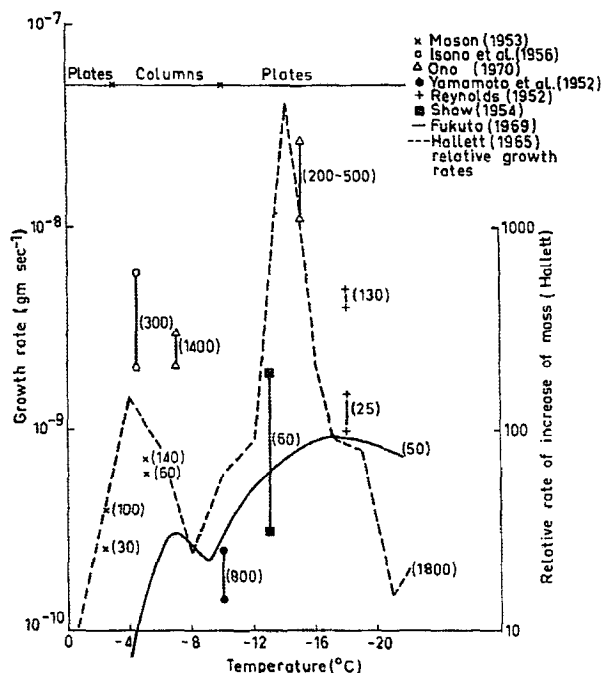


FIG. 1. Available experimental data on the growth rates of ice crystals. The times of growth (sec) are shown in parentheses. The growth is at water saturation except for Yamamoto *et al.* (1952) where 97% saturation with respect to water is indicated. Hallett's curve is not strictly comparable with the other data as his observations were made in a diffusion cloud chamber.

¹ Present affiliation: Geophysical Institute, University of Alaska, College, Alaska.

calculations and experimental values were made by Reynolds (1952), Yamamoto *et al.* (1952), Mason (1953), Isono *et al.* (1956) and Fukuta (1969).

Koenig (1968) computed the growth of larger crystals, supplementing the diffusion term by a ventilation contribution due to the crystal motion. He was able to generate the peaks in the growth rates observed by Hallett at -5 and -15°C , by choosing suitable values for the axial ratios and densities.

Now that more reliable values of axial ratios of ice crystals have become available (Ono, 1970), we can apply these to calculate the growth of ice crystals as a function of time and temperature.

2. Equations for computation of growth rates

Equations for the mass and heat transfer for ventilated spherical particles are readily available in the literature. For other shapes these equations can be modified on the basis of the available experimental and theoretical results on the mass and heat transfer for simple shapes such as spheroids, discs, cylinders and cubes, and such results can be extended with further modification if necessary for the more complex shapes. Since ice crystals are broadly divisible into the two growth habits, columnar and plate-like, few assumptions are necessary.

For stationary bodies of most shapes, the mass and heat transfer rate equations may be written as

$$\frac{dm}{dt} = 4\pi CD(\rho_s - \rho_\infty), \tag{2.1}$$

$$\frac{dH}{dt} = 4\pi CK(T_s - T_\infty), \tag{2.2}$$

where the capacity C allows for the shape of the crystal.²

The enhancement of the growth rate by ventilation is derived in a manner indicated by Koenig (1968). For ventilated bodies, the mass and heat transfers are expressed in terms of Sherwood and Nusselt numbers by

$$\frac{dm}{dt} = \text{Sh} \frac{AD}{L^*} (\rho_s - \rho_\infty), \tag{2.3}$$

$$\frac{dH}{dt} = \text{Nu} \frac{AK}{L^*} (T_s - T_\infty). \tag{2.4}$$

In general, the values of Sherwood and Nusselt numbers depend on the definition of the characteristic length L^* . Pasternak and Gauvin (1960) and Skelland and Cornish (1963) found that if L^* is defined as the ratio of the total surface area A divided by its perimeter P normal to the flow, then their results for Sherwood and Nusselt numbers and those of the other workers can be represented by two relations, which, within the

² See the Appendix for a complete list of symbols.

accuracy of their experiments, can be reduced to

$$\left. \begin{aligned} \text{Sh} &= (\text{Sh})_0 + 0.7 \text{Sc}^{\frac{1}{3}} \text{Re}_L^{*\frac{1}{2}} \\ \text{Nu} &= (\text{Nu})_0 + 0.7 \text{Pr}^{\frac{1}{3}} \text{Re}_L^{*\frac{1}{2}} \end{aligned} \right\} \tag{2.5}$$

where $(\text{Sh})_0$ and $(\text{Nu})_0$ correspond to the values of Sherwood and Nusselt numbers for no ventilation, and can be readily obtained by comparing Eqs. (2.1) and (2.2) with (2.3) and (2.4), respectively; in so doing we find

$$(\text{Sh})_0 = (\text{Nu})_0 = \frac{4\pi CL^*}{A}. \tag{2.6}$$

Unfortunately, these data cover axial ratios < 3 , far smaller than those observed for ice crystals. For plate-like crystals, some justification for using Eqs. (2.5) for higher axial ratios is seen from the values of "wind factors" for mass and heat transfer for evaporating crystals obtained by Thorpe and Mason (1966). These values, which are one-half the Sherwood and Nusselt numbers, are not very different from the values from Eqs. (2.5). For cylinders a comparison is possible with results for very long cylinders, for which these expressions reduce to

$$\begin{aligned} \text{Sh} &= (\text{Sh})_0 + 0.87 \text{Sc}^{\frac{1}{3}} \text{Re}_d^{\frac{1}{2}}, \\ \text{Nu} &= (\text{Nu})_0 + 0.87 \text{Pr}^{\frac{1}{3}} \text{Re}_d^{\frac{1}{2}}. \end{aligned}$$

Experimental values of the Nusselt numbers for long cylinders (Fishenden and Saunders, 1965) are not far from the numbers given by these relations for Reynolds numbers from about 1 to 100.

Therefore, it is reasonable to assume the validity of Eqs. (2.5) for axial ratios common in natural ice crystals.

From Eqs. (2.5) we have

$$\text{Sh} = \frac{4\pi CL^*}{A} \left(1 + 0.7 \frac{A}{4\pi CL^*} \text{Sc}^{\frac{1}{3}} \text{Re}_L^{*\frac{1}{2}} \right), \tag{2.7}$$

$$\text{Nu} = \frac{4\pi CL^*}{A} \left(1 + 0.7 \frac{A}{4\pi CL^*} \text{Pr}^{\frac{1}{3}} \text{Re}_L^{*\frac{1}{2}} \right). \tag{2.8}$$

For water vapor in air $\text{Sc}^{\frac{1}{3}} = \text{Pr}^{\frac{1}{3}} \approx 0.9$, and since by definition $L^* = A/P$,

$$\text{Sh} = \text{Nu} = \frac{4\pi CL^*}{A} \left(1 + 0.6 \frac{P}{4\pi C} \text{Re}_L^{*\frac{1}{2}} \right).$$

Substituting for Sh and Nu in Eqs. (2.3) and (2.4), we have

$$\frac{dm}{dt} = 4\pi CD(\rho_s - \rho_\infty) \left(1 + 0.6 \frac{P}{4\pi C} \text{Re}_L^{*\frac{1}{2}} \right), \tag{2.9}$$

$$\frac{dH}{dt} = 4\pi CK(T_s - T_\infty) \left(1 + 0.6 \frac{P}{4\pi C} \text{Re}_L^{*\frac{1}{2}} \right). \tag{2.10}$$

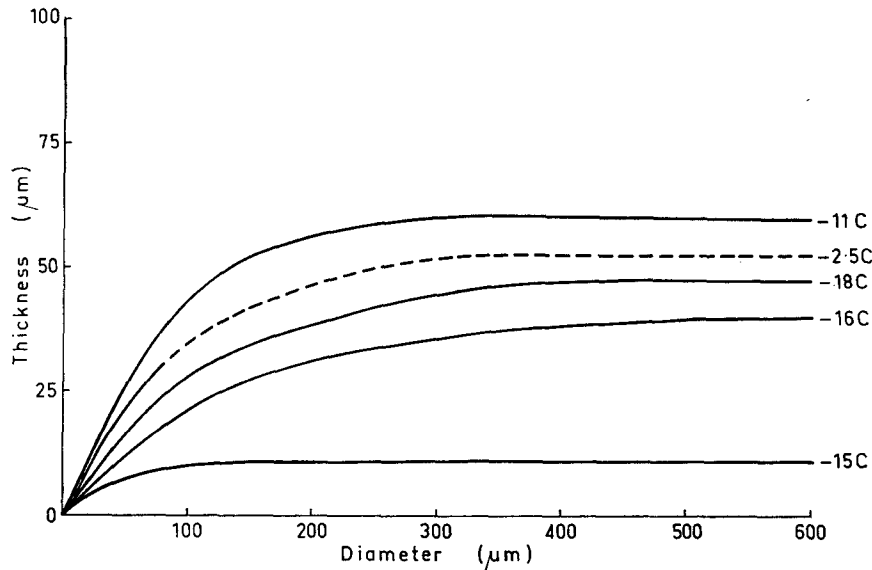


FIG. 2. Mean experimental growth modes of plate-like crystals at various temperatures (after Ono, 1970). The dotted line is the assumed extrapolation at -2.5°C .

Proceeding in the same way as for the unventilated case derived by Mason (1953), we obtain for the growth rate of a freely falling ice crystal

$$\frac{dm}{dt} = 4\pi \frac{\sigma}{f(T)} \left(C + \frac{P}{4\pi} 0.6 \text{Re}_L^{*3/2} \right), \quad (2.11)$$

where

$$f(T) = \frac{JL_s^2 M}{KRT^2} + \frac{RT}{DMP_s(T)}.$$

This expression for the growth rate of ice crystals is similar to that obtained by Koenig (1968), but is simpler to compute because of the approximate equality of Sherwood and Nusselt numbers. Eq. (2.11) illustrates how the growth rate is made up of two terms, involving diffusion and ventilation, respectively.

Let us now consider the appropriate values of the various parameters in the above equation.

a. Axial ratios

The available information on axial ratios of crystals at various growth temperatures has been gathered together by Ono (1970), whose curves for plate-like crystals are shown in Fig. 2. These curves apply to the following crystal types:

- (i) solid hexagonal plates grown at -2.5°C (Mason, 1953),
- (ii) thick hexagonal plates grown at -11°C (Ono, 1970),
- (iii) plane dendritic crystals grown at -15°C [observations by Nakaya and Terada (1935) on millimeter-sized crystals extrapolated to smaller sizes by Ono (1970)],

- (iv) plates with sector-like extensions grown at -16°C (Reynolds, 1952),
- (v) solid hexagonal plates grown at -18°C (Reynolds, 1952).

The axial ratios for columnar crystals are shown in Fig. 3. These are Ono's (1970) mean values for the three categories, needle (growth temperature -5°C), sheath (-7°C), and solid/hollow column (-9°C).

b. Capacity

1) HEXAGONAL PLATE-LIKE CRYSTALS

The capacity of a plate-like crystal can be closely approximated by that of an oblate spheroid of eccentricity $e = h/d$; thus,

$$C_p = \frac{0.5(1-e^2)^{3/2}}{\sin^{-1}(1-e^2)^{1/2}} d = f(e)d, \quad (2.12)$$

where h is the thickness of the plate and d the equivalent diameter, i.e., the diameter of a circle of the same area.

McDonald (1963) has shown that these C values may be applied to the more intricate plane crystals such as dendritic shapes without large error. They may be treated as solid hexagonal plates of the same diameter and thickness with at most an error of 20%.

2) HEXAGONAL COLUMNAR CRYSTALS

The capacity of a column may be taken to be that of a prolate ellipsoid of eccentricity $e = d/L$; in this case, we have

$$C_c = \frac{0.5(1-e^2)^{3/2}}{\ln \left[\frac{1+(1-e^2)^{1/2}}{e} \right]} L, \quad (2.13)$$

where L is the length of the column and d the "equivalent diameter" of the basal plane, i.e., the diameter of a circle of the same area.

Whether the columns are solid hexagonal prisms, sheaths or needles, their capacities may be satisfactorily approximated by the above equation.

c. Reynolds number

For discs and cylinders of any given dimension the Reynolds number at terminal velocity can be obtained from the curves given by Jayaweera and Cottis (1969). These Reynolds numbers will be expressed in terms of the equivalent diameter d , rather than Re_{L^*} used in (2.11). We must therefore express Re_{L^*} in terms of Re_d . We also consider below the ventilation factor which must be introduced in (2.11) when we are dealing with intricate crystal shapes.

1) PLATES

We express L^* in terms of the equivalent diameter d (for solid discs) as

$$L^* = \frac{\frac{\pi d^2}{2} + \pi d l}{\pi d} = \frac{d}{2}(1 + 2e).$$

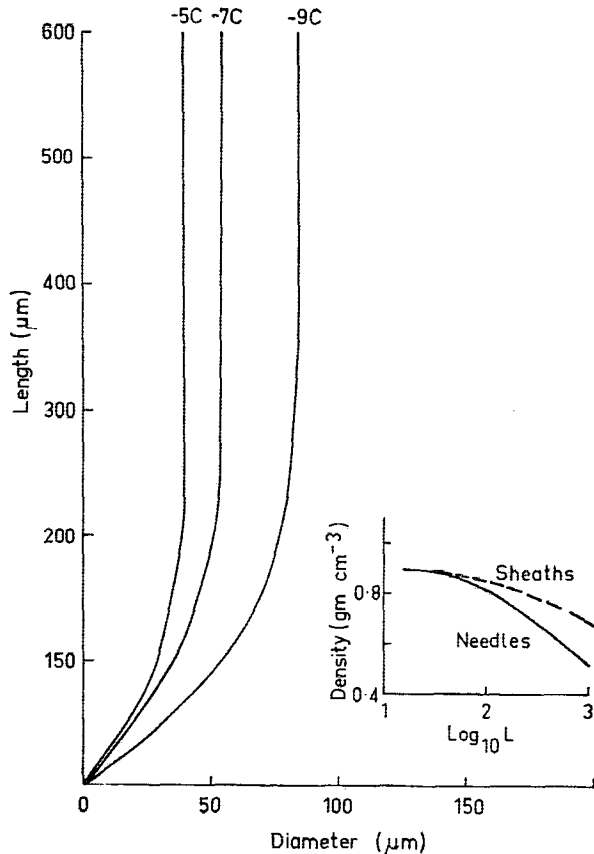


FIG. 3. Mean experimental growth mode of columnar crystals at temperatures corresponding to needles, sheaths and hollow/solid columns observed by Ono (1970). Inset: The density of needles and sheaths as a function of their lengths (Ono, 1970).

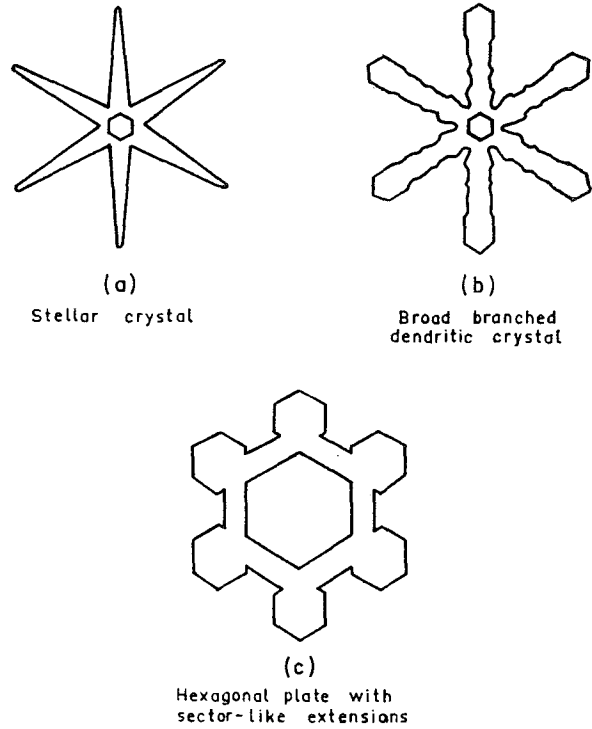


FIG. 4. Examples of stellar crystals, a., broad-branched dendritic crystals, b., and hexagonal plates with sector-like extension, c.

Hence,

$$Re_{L^*} = 0.5(1 + 2e) Re_d. \tag{2.14}$$

When we are no longer dealing with solid crystals but with branched forms such as plane dendrites, the ventilation term in (2.11) must be increased by a factor Y . This may be determined as follows.

Rewriting the ventilation term in (2.11) as

$$\frac{4\pi\sigma}{f(T)} F', \text{ where } F' \propto P Re_{L^*}^{\frac{1}{2}},$$

and since

$$Re_{L^*} = \frac{VL^*}{\nu} = \frac{VA}{\nu P},$$

where ν is a constant for a given temperature, then

$$F' \propto (VA P)^{\frac{1}{2}}. \tag{2.15}$$

From the work of Jayaweera and Cottis (1969), it appears that the terminal velocities of plane dendrites can be taken to be the same as those of solid plates of the same mass and thickness. We can therefore assume that the ventilation factor for crystals having the same surface area and mass is proportional to the square root of the perimeters normal to the flow; thus,

$$Y = \left(\frac{P}{\pi d} \right)^{\frac{1}{2}}. \tag{2.16}$$

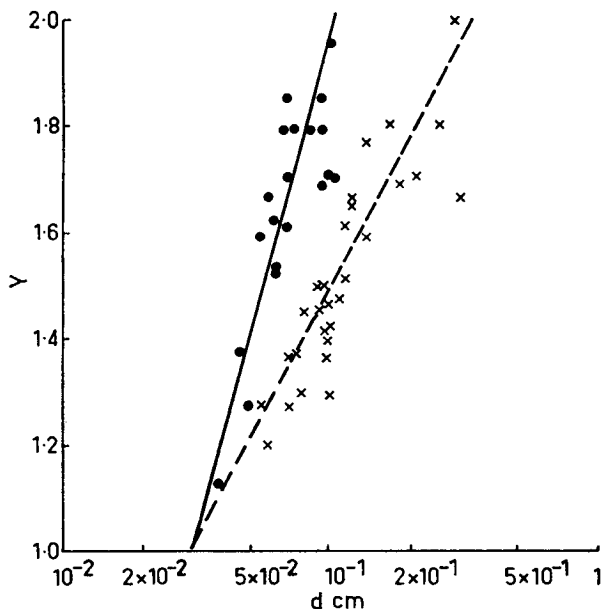


FIG. 5. The shape factor Y for dendritic/stellar (circles) and sector-like crystals (crosses) as a function of the diameter d of a disc having the same surface area of cross section as the crystal.

In the present computations we need to know what value of Y to adopt for plane crystals grown at -15 and -16°C . To determine suitable values we have assumed that the dendritic crystals characteristic of -15°C take the common forms of stellar and broad-branched crystals illustrated in Figs. 4a and b. Many measurements of the perimeter and surface area of crystals of these shapes were made from the micrographs given by Nakaya (1954).

In the case of -16°C computations, similar determinations of Y were made for hexagonal plates with sector extensions (Fig. 4c), since this shape agrees best with that illustrated by Reynolds (1952).

The values of Y calculated from these measurements are plotted as a function of d in Fig. 5, the lines of best fit being

$$Y = 1.0 + 0.8 \ln[(d/3) \times 10^{-2}] \quad \text{for dendrites/stellar,} \quad (2.17)$$

$$Y = 1.0 + 0.4 \ln[(d/3) \times 10^{-2}] \quad \text{for sectors.} \quad (2.18)$$

2) COLUMNS

Here again it is convenient to define the Reynolds number in terms of the equivalent diameter rather than L^* . For cylinders we have

$$L^* = \frac{\frac{\pi d^2}{2} + \pi dL}{2(d+L)} = \frac{\pi}{4} d \left(1 + \frac{1}{1+e} \right).$$

Hence

$$\text{Re}_{L^*} = \frac{\pi}{4} \left(1 + \frac{1}{1+e} \right) \text{Re}_d.$$

d. Density

1) PLATES

When a plate-like crystal is replaced by an equivalent disc having the same mass, thickness and surface area, the density of this disc will not differ from that of solid ice unless the crystals have hollow internal structures. Since such growth is rare at water saturation, the density of plate-like crystals is assumed to be 0.9 gm cm^{-3} in the present calculations. Mean experimental growth modes were shown in Fig. 2 (after Ono, 1970).

2) COLUMNS

For columns, on the other hand, hollow structures are a common occurrence; hence, the density of the equivalent cylinder could be less than that of pure ice. Ono (1970) has deduced the bulk densities of various types of columnar crystals as a function of their size and finds that only needle and sheath-type crystals show a marked decrease in density with length. Therefore, in these calculations the density of needles and sheaths is assumed to decrease with length according to the curves given by Ono (1970), which were reproduced in the inset of Fig. 3. The densities of solid/hollow columns are assumed to be 0.9 gm cm^{-3} .

3. Comparison between rates of growth by diffusion and ventilation

It is of interest to compare the relative contributions of diffusion and ventilation to the growth of ice crystals falling at terminal velocity under conditions of water saturation.

a. Plate-like crystals

Substituting for C , P and Re_{L^*} in the equation for the growth rate [(2.11)], we have

$$\begin{aligned} \frac{dm}{dt} &= \frac{4\pi\sigma}{f(T)} \{ f(e)d + 0.11Yd[\text{Re}_d(1+2e)^{\frac{1}{2}}] \}, \\ &= \frac{4\pi\sigma}{f(T)} d [f(e) + F], \end{aligned} \quad (3.1)$$

where

$$\left. \begin{aligned} f(e) &= \frac{0.5(1-e^2)^{\frac{1}{2}}}{\sin^{-1}(1-e^2)^{\frac{1}{2}}} \\ F &= 0.11Y[\text{Re}_d(1+2e)^{\frac{1}{2}}] \end{aligned} \right\}$$

The relative contributions of diffusion and ventilation to the growth rate of plane crystals are illustrated by a comparison of the magnitudes of $f(e)$ and F as shown in Fig. 6 for solid hexagonal plates ($Y=1$). From this figure it is evident that the growth rate is dominated by the ventilation term once the crystal exceeds a diameter of $\sim 300 \mu\text{m}$.

For comparison purposes we have also calculated the ventilation term for a dendritic crystal of thickness 10 μm using values of *Y* given by Eq. (2.17). This is shown as the dotted line in Fig. 6, which illustrates how the dendritic shape enhances the ventilation growth rate as compared with that of a solid plate.

b. Columns

The relative effects of ventilation and diffusion on the growth of columns can be similarly expressed by the growth rate equation

$$\frac{dm}{dt} = \frac{4\pi\sigma L}{f(T)} [f(e) + F], \tag{3.2}$$

where

$$f(e) = \frac{0.5(1 - e^2)^{\frac{1}{2}}}{\ln \left[\frac{1 + (1 - e^2)^{\frac{1}{2}}}{e} \right]}$$

$$F = 0.085(1 + e) \left[\text{Re}_d \left(1 + \frac{1}{e+1} \right) \right]^{\frac{1}{2}}$$

The values of *f*(*e*) and *F* are compared in Fig. 7 for different values of column diameters. In these calculations the density is assumed to be 0.9 gm cm⁻³. The effect of using the lower densities given by Ono (1970) for needles once they have reached a few hundred microns is to decrease the fall velocity and hence the relative contribution of the ventilation component of

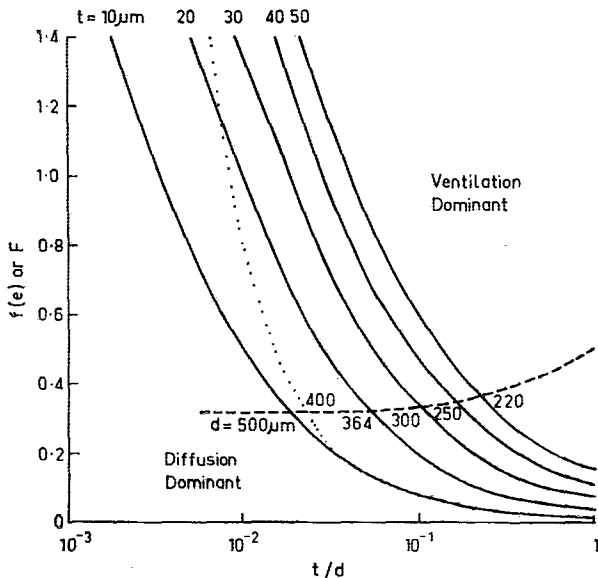


FIG. 6. Comparison of ventilation (solid lines) and diffusion (dashed line) effects on the growth of plate-like ice crystals; the dotted curve corresponds to ventilation for 10 μ thick plate with shape factor *Y* corresponding to dendritic growth. The annotated values of diameter are those for which the two effects are equal.

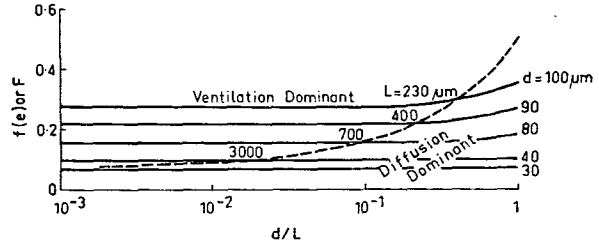


FIG. 7. Comparison of ventilation (solid lines) and diffusion (dashed line) effects on the growth of columnar crystals. The annotated values of length are those for which the two effects are equal.

growth. However, even for the extreme case cited, the decrease will only amount to ~20%.

In contrast to the plate case, the ventilation term in the case of columns never becomes overwhelmingly large as compared with the diffusion term. Diffusion is, of course, dominant in the early stages of growth, and ventilation only becomes more important for comparatively long columns of diameter >40 μm.

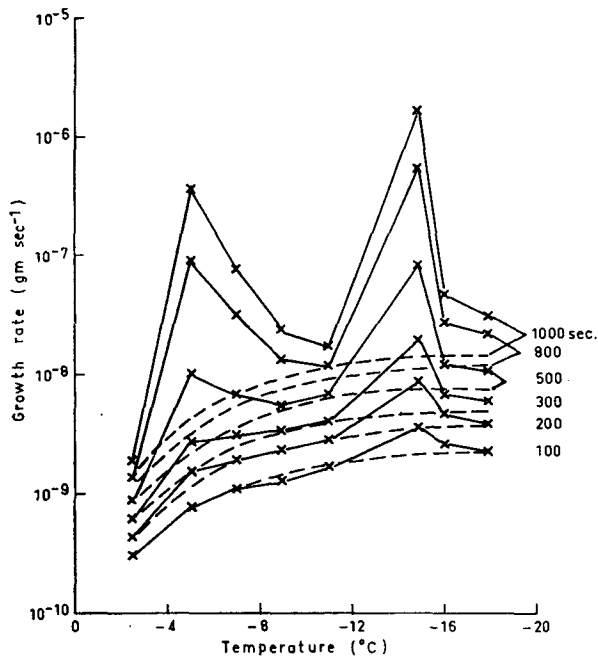
4. Rate of growth of ice crystals

The growth rate Eq. (2.11), together with the experimental curves of the axial ratios, the density values and the shape factors, can be used to calculate the growth rate and hence the mass of the crystals at different intervals of time. Because the axial ratios are known only for particular temperatures, calculations were made only at -5, -7, -9C for columns and at -2.5, -11, -15, -16 and -18C for plate-like crystals.

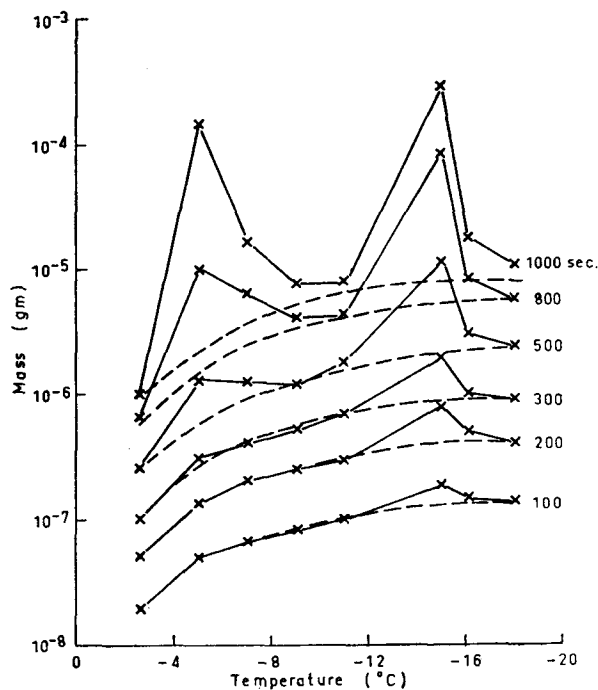
The initial length of the major axis of the crystal was taken as 1 μm and the time required for the crystal to increase in length by definite steps was calculated. At each step the length of the other axis was determined from the experimental axial ratio curves (Figs. 2 and 3). The increment in length was 1 μm for the first 200 μm and 2 μm thereafter. These increments were sufficiently small for masses of crystals after 200 sec to be within 5% of those which could be obtained with lower increments.

The masses of the crystals and the rates of growth of crystals growing in air at water saturation at the temperatures mentioned and falling at their terminal velocities relative to air are shown in Figs. 8a and b for growth times in steps from 100 to 1000 sec. The figures also show the growth of a spherical ice crystal under identical conditions with an initial diameter of 1 μm.

The mass to which a crystal grows does not differ appreciably from that of an ice sphere up to ~300 sec, and only after 500 sec of growth does the mass of the crystals corresponding to -5C begin to show appreciably higher values. At -15C, however, a peak in the growth rate is observed very early in the growth. This is due to the very small thickness of 11 μm assumed for dendritic crystals growing at this temperature, which gives rise to a high axial ratio very early in



a.



b.

FIG. 8. Isochrones for the growth rate, a., and mass, b., of ice crystals growing in different habit ranges with the temperature, pressure following the moist adiabatic curve. (The atmospheric pressures at 0, -10 and -20°C were 850, 700 and 600 mb, respectively.) The crosses refer to plate-like and columnar ice crystals, while the dashed lines are for an ice sphere.

the growth. The inference from these results is that high growth rate is a consequence of high axial ratios. For low axial ratios the initial shape has only secondary

importance while the growth is mainly influenced by the vapor pressure difference between the crystal and the environment.

The growth of axes of columnar crystals may be used to determine the time that elapses before the crystals grow to a size capable of riming. In Fig. 9 isochrones are drawn on an axial-length diagram for columns. When compared with the boundary curve for rimed and unrimed crystals given by Ono (1969), these suggest that the crystals grow to a size capable of riming in ~ 400 sec. Since the growth of columnar crystals does not deviate appreciably from that of ice spheres until about this time of growth, it may be sufficient to use a spherical model to calculate the time required for crystals to grow to sizes capable of riming. This is useful since the observations of Mossop and Ono (1969) on the number of ice crystals in clouds suggest riming as a possible process for ice multiplication.

The time required for plate-like crystals to reach sizes capable of growth by riming can be estimated

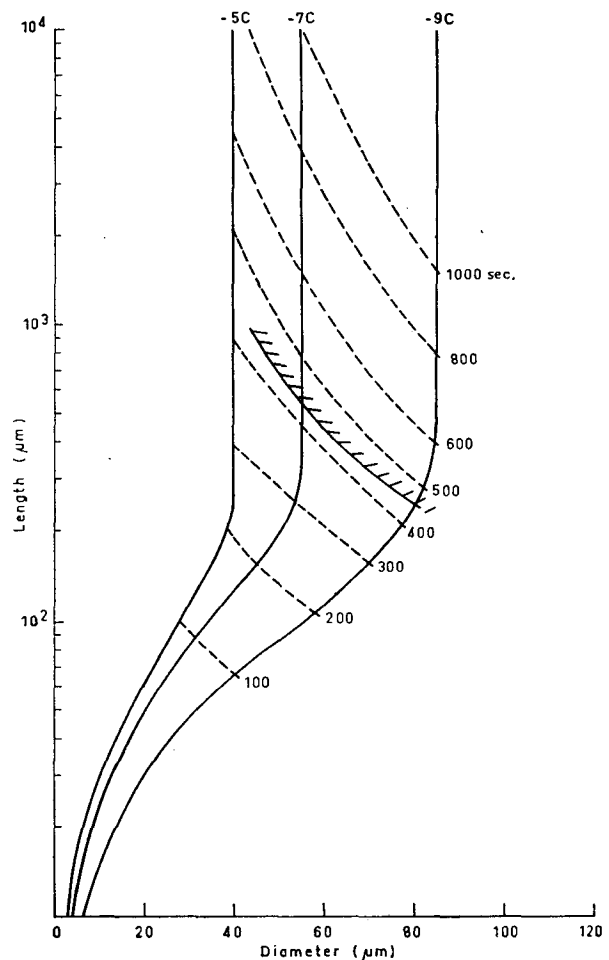


FIG. 9. Growth of axes of columns. Isochrones (dashed lines) and axial-length growth relations (solid lines) are shown at various temperatures. The hatched overlay is the boundary curve for the onset of riming.

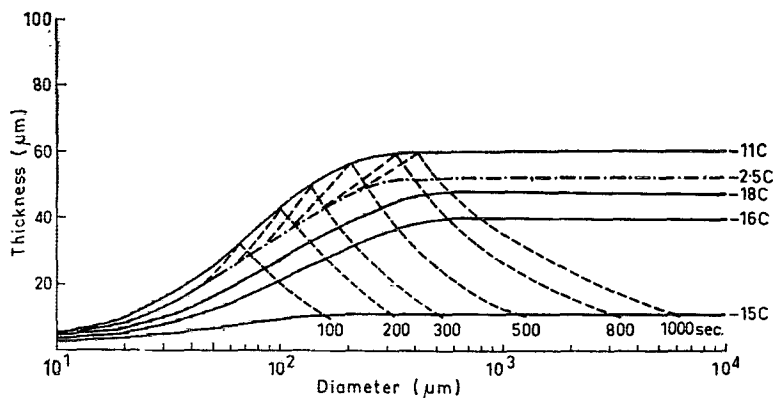


FIG. 10. Isochrones (dashed lines) and thickness-diameter growth relations (solid lines) at various temperatures for plate-like crystals.

only in the cases of hexagonal plates. These have to have a diameter $> 300 \mu$ for appreciable numbers of water drops to be swept up (Ono, 1969; Auer and Wilkins, 1970). From Fig. 10 we see that at -11 and -18 C, where hexagonal plates are found, the required growth times would be 800 and 500 sec, respectively.

5. Discussion

The present calculations of the growth rates and the masses to which the ice crystals grow after different times of growth at water saturation indicate that these quantities depend very much on the size and shape of the crystal. However, in the initial stages up to about 300 sec the controlling factor is the vapor pressure difference between the environment and the crystal, the effect of shape being small enough to use a spherical model for calculating the growth.

For later stages of growth the crystal geometry plays a major role in influencing the growth rate. The peaks in the growth rate at about -5 and -15 C are associated with high axial ratios.

Hallett's (1965) curve for the relative growth rate at a variety of temperatures is misleading in that it applies to the average growth rate over a long period of time in a diffusion cloud chamber. It cannot, therefore, be applied to all sizes of crystal growth in cloud, as was assumed by Neumann *et al.* (1968).

We should emphasize two possible sources of error in these computations. In our adopted values of the axial ratios we have followed Ono (1970). He found, for both plane crystals and columns, that growth along the minor axis virtually ceases once the major axis exceeds a certain length. There is evidence that this may not be entirely true. For instance, in the case of needles grown at -5 C, Ono (1970) indicates that the minor axes cease growing at $\sim 50 \mu\text{m}$. However, his observations were confined to needles less than $600 \mu\text{m}$ long. Photographs published by Nakaya (1954) and Magono and Lee (1966) suggest that needles 1 mm long may have diameters up to $80 \mu\text{m}$.

Since the peaks in growth rate are primarily due to the high axial ratios, any reduction in the ratios will have the effect of smoothing out the peaks somewhat. It is obvious that further determinations of growth mode at larger sizes and at other growth temperatures are urgently needed.

The second major uncertainty is the assumption that the vapor pressure is constant over the crystal surface. This rests upon the assumption that the temperature over the surface of the growing crystal is uniform, an assumption for which McDonald (1963) has put forward supporting arguments. The lines of electric field near a conductor are concentrated toward edges and corners; hence, by analogy, one would expect that the vapor flux to a crystal would be concentrated toward the minor faces. The flux toward the central region of major faces would be comparatively small, increasing as one approached the boundary edges. Considering the small migration distances ($\leq 5 \mu\text{m}$) of molecules upon the surface of an ice crystal (Mason *et al.*, 1963), it is difficult to understand why, for instance, long columns do not grow in a "dog-bone" shape with some thickening of the ends of the column relative to the middle. The basic assumption of surface temperature uniformity therefore requires re-examination.

Acknowledgments. The author wishes to express his thanks to Mr. J. Warner, to Drs. S. C. Mossop, T. L. Ogden, A. Ono and J. L. Brownscombe for their comments and suggestions, and particularly to Dr. S. C. Mossop, who read the manuscript and offered many valuable comments. Mrs. F. Brackenbury assisted in the preparation of the computing program for the CDC 3200.

APPENDIX

List of Symbols³

m	mass of crystal
H	heat

³ All symbols are in cgs units.

L_s	latent heat of sublimation of ice
C	electrostatic capacity
D	diffusion coefficient of water vapor in air
K	thermal conductivity of air
ρ	vapor density
T	temperature
A	total surface area
L^*	characteristic dimension
Nu	Nusselt number
Sh	Sherwood number
Pr	Prandtl number, $c_p\mu/K$
Sc	Schmidt number, ν/D
Re	Reynolds number, Vd/ν
$P_e(T)$	saturation vapor pressure over a plane ice surface at temperature T
σ	supersaturation of the environment relative to ice
R	gas constant
J	Joule constant
M	molecular weight of ice
d	diameter of the circle having the same area as the basal face of the crystal
h	thickness of plate
L	length of the major axis of column
e	ratio of minor to major axis
ν	kinematic viscosity of air
t	time
V	fallspeed of crystal
μ	dynamic viscosity of air
c_p	specific heat of air at constant pressure
P	perimeter of the crystal normal to the direction of fall

Subscripts

S	value at surface of crystal
∞	ambient value
L^*	defined in terms of L^*
d	defined in terms of d
0	value at zero velocity or zero Reynolds number

REFERENCES

- Auer, A. J., Jr., and R. D. Wilkins, 1970: Riming properties of natural ice crystals. *Preprints of Papers, Conf. Cloud Phys.*, Fort Collins, Colo., Amer. Meteor. Soc., 81-82.
- Fishenden, M., and O. A. Saunders, 1965: *An Introduction to Heat Transfer*. Oxford, Clarendon Press, p. 129.
- Fukuta, N., 1969: Experimental studies on the growth rate of small ice crystals. *J. Atmos. Sci.*, **26**, 522-531.
- Hallett, J., 1965: Field and laboratory observation of ice crystal growth from the vapor. *J. Atmos. Sci.*, **22**, 64-69.
- Houghton, H. G., 1950: A preliminary quantitative analysis of precipitation mechanisms. *J. Meteor.*, **7**, 363-369.
- Isono, K., M. Kumbayasi, Y. Yamanaka and H. Fujita, 1956: An experimental investigation of the growth of ice crystals in a supercooled fog. *J. Meteor. Soc. Japan, Ser. 2*, **34**, 34-39.
- Jayaweera, K. O. L. F., and R. E. Cottis, 1969: The fall velocities of plate-like and columnar ice crystals. *Quart. J. Roy. Meteor. Soc.*, **95**, 703-709.
- Koenig, L. R., 1968: Numerical modeling of ice deposition. Memo. RM-5715-NSF, The Rand Corporation, Santa Monica, Calif.
- McDonald, J. E., 1963: Use of electrostatic analogy in studies of ice crystal growth. *Z. Angew. Math. Phys.*, **14**, 610-619.
- Magono, C., and C. W. Lee, 1966: Meteorological classification of natural snow crystals. *J. Fac. Sci. Hokkaido Univ., Ser. 7*, **2**, 321-335.
- Mason, B. J., 1953: The growth of ice crystals in a supercooled water cloud. *Quart. J. Roy. Meteor. Soc.*, **79**, 104-111.
- , G. W. Bryant and A. P. van den Heuvel, 1963: The growth habits and surface structure of ice crystals. *Phil. Mag.*, **8**, 505-526.
- Mossop, S. C., and A. Ono, 1969: Measurements of ice crystal concentrations in clouds. *J. Atmos. Sci.*, **26**, 130-137.
- Nakaya, U., 1954: *Snow Crystals*. Harvard University Press, 317-377.
- , and T. Terada, Jr., 1935: Simultaneous observations of mass, fall velocities and form of individual snow crystals. *J. Fac. Sci. Hokkaido Univ., Ser. 2*, **1**, 191-201.
- Neumann, J., K. R. Gabriel and A. Gagin, 1968: Cloud seeding and cloud physics in Israel: Results and problems. *Proceedings of the Conference on Water for Peace*, Vol. 2., Washington, D. C., Gov't. Printing Office, 375-388.
- Ono, A., 1969: The shape and riming properties of ice crystals in natural clouds. *J. Atmos. Sci.*, **26**, 138-147.
- , 1970: Growth modes of ice crystals in natural clouds. *J. Atmos. Sci.*, **27**, 649-658.
- Pasternak, I. S., and W. H. Gauvin, 1960: Turbulent heat and mass transfer from stationary particles. *Can. J. Chem. Eng.*, **38**, 35-42.
- Reynolds, S. E., 1952: Ice crystal growth. *J. Meteor.*, **9**, 36-40.
- Skelland, A. H. P., and A. R. H. Cornish, 1963: Mass transfer from spheroids to an air stream. *AIChE J.*, **9**, 73-76.
- Thorpe, A. D., and B. J. Mason, 1966: The evaporation of ice spheres and ice crystals. *Brit. J. Appl. Phys.*, **17**, 541-548.
- Todd, C., 1964: A system for computing ice phase hydrometeor development. Rept. ARG 64, Pa-121, Meteorology Research Inc., Calif., 30 pp.
- Yamamoto, G., S. Ogiwara, K. Yoshida, A. Muira, T. Okita and T. L. Ohtake, 1952: Observations of the rate of growth of ice crystals artificially produced in the atmosphere. *Tohoku Univ. Sci. Rept.*, **4**, 83-87.